Journal of Materials Chemistry

Cite this: J. Mater. Chem., 2011, 21, 8653

www.rsc.org/materials

PAPER

Cyclometallated platinum(II) complexes of 1,3-di(2-pyridyl)benzenes for solution-processable WOLEDs exploiting monomer and excimer phosphorescence†‡

Wojciech Mróz,*[a] Chiara Botta,[a] Umberto Giovanella,[a] Ester Rossi,[b] Alessia Colombo,[b] Claudia Dragonetti,[b] Dominique Roberto,*[bc] Renato Ugo,[b] Adriana Valore[c] and J. A. Gareth Williams*[d]

Received 13th January 2011, Accepted 31st March 2011
DOI: 10.1039/c1jm10193e

Two cyclometallated platinum(II) complexes, *N^C^N*-5-fluoro-1,3-di(2-pyridyl)benzene platinum(II) chloride, **FPtCl**, and *N^C^N*-5-methyl-1,3-di(2-pyridyl)benzene platinum(II) isothiocyanate, **MePtNCS**, have been synthesized and characterized. Both complexes are highly efficient phosphorescent green emitters which can also display excimer emission in the red region. They have been studied as triplet emitters in solution-processed, multilayer organic light-emitting diodes (OLEDs), together with the known complex of 5-methyl-1,3-di(2-pyridyl)benzene, **MePtCl**, for comparison. The trend in efficiencies of the OLEDs prepared correlates with the charge-trapping properties of the complexes. The most efficiently emitting complex, FPtCl, was used as the dopant in a solution-processed white OLED, employing monomer and excimer emission.

Introduction

To construct efficient organic light-emitting diodes (OLEDs), emitters possessing high quantum efficiencies under electrical operation are required. Since the introduction of phosphorescent metal complexes into this field, which utilize both singlet and triplet excitons to generate electroluminescence (EL),[1] many new phosphorescent materials have been synthesized for potential OLED applications.[2,3] Among them, a class of cyclometallated platinum(II) complexes with *N^C^N*-coordinated 1,3-di(2-pyridyl)benzene ligands is gaining increasing interest, owing to their high emission phosphorescence quantum yields.[4–7] These compounds have been tested as phosphors in multilayer OLEDs, leading to high external quantum efficiencies.[8,9] Additionally, owing to their propensity to form highly emissive bimolecular excimers or aggregates, they are of particular interest for the production of white OLEDs (WOLEDs). The combination of efficient triplet monomer and excimer emission to generate broad-band light across the visible spectrum has been put forward as an attractive route to single-dopant white-emitting devices.[10] WOLEDs are expected to be more efficient and less expensive than fluorescent and incandescent illumination light sources.[11,12]

They also offer useful properties like tunable correlated colour temperature (CCT) and can be obtained as completely flexible large area devices.[13,14] Excimers possess a broad EL spectrum, a desirable feature for illumination purposes as it increases the colour rendering index (CRI). Moreover, among many strategies for obtaining white light from organic or organometallic molecular materials, excimer emission is of particular interest as it allows simplified device architectures to be used. This is because excimers lack a bound ground state and, as a result, energy transfer between multiple dopants is significantly reduced.[15]

Most examples of devices with phosphorescent excimer emission use cyclometallated platinum(II) complexes with bidentate, *N^C*-coordinating aryl-pyridines and β-diketonate co-ligands.[10,15–17] Based on the same principle, WOLEDs with *N^C^N* coordinated platinum(II) complexes have since been created.[18] Further improvements in device performance were recently achieved by combining the monomer and excimer emission of such complexes with exciplex emission involving the host material.[19] However, until now, all such excimer WOLEDs have been vacuum-sublimed multilayer structures. Such fabrication methods, based on evaporation, are generally expensive

[a]*Istituto per lo Studio delle Macromolecole, Consiglio Nazionale delle Ricerche, via Bassini 15, 20133 Milano, Italy. E-mail: w.mroz@ismac.cnr.it*
[b]*Dip. di Chimica Inorganica, Metallorganica e Analitica "Lamberto Malatesta" dell'Università degli Studi di Milano and UdR INSTM di Milano, via Venezian 21, 20133 Milano, Italy. E-mail: dominique.roberto@unimi.it*
[c]*Istituto di Scienze e Tecnologie Molecolari, Consiglio Nazionale delle Ricerche, Via Venezian 21, 20133 Milano, Italy*
[d]*Department of Chemistry, University of Durham, Durham DH1 3LE, UK. E-mail: j.a.g.williams@durham.ac.uk*

† Dedicated to the memory of Professor Jan Kalinowski, a pioneer of electroluminescence, deceased 18 December 2010.

‡ Electronic supplementary information (ESI) available: IR and NMR characterization of the complexes, contrasting influence of F atoms, influence of PVK electromer and AFM data. See DOI: 10.1039/c1jm10193e

processes, requiring precise control of evaporation rates when two or more compounds are in the same layer (*e.g.* host and dopant), and are less suitable for the production of large area devices due to the higher cost.

In this contribution, we present electroluminescent devices that use Pt(*N^C^N*)X complexes as phosphors, built by a simple spin-coating technique. Two complexes have been investigated, as shown in Chart 1: *N^C^N*-5-fluoro-1,3-di(2-pyridyl)-benzene platinum(II) chloride, **FPtCl**,[7] and *N^C^N*-5-methyl-1,3-di-(2-pyridyl)-benzene platinum(II) isothiocyanate, **MePtNCS**. The known chloro analogue of the latter complex, **MePtCl**,[5] has also been studied for comparison. The synthesis and photophysical properties of the complexes are reported, together with studies of their use as phosphors in spin-coated diodes. Finally, the complex showing the best performance has been applied in a WOLED employing monomer and excimer emission mechanisms, in a simple solution-processed multilayer device.

Experimental

General comments

Reagents were purchased from Sigma-Aldrich or Fluorochem. Products were characterized by elemental analysis, mass spectrometry (FAB^+ and MALDI-TOF) and by ^1H and ^{13}C NMR spectroscopy (Bruker Avance DRX-400 instrument). ^1H NMR spectra are referenced relative to residual proton solvent resonances; δ are in ppm and coupling constants in Hz. 5-Methyl-1,3-di(2-pyridyl)benzene was prepared as reported.[5]

Synthesis of 5-fluoro-1,3-di(2-pyridyl)benzene

A mixture of commercial 1,3-dibromo-5-fluorobenzene (0.279 g, 1.10 mmol), 2-(tri-*n*-butylstannyl)pyridine (1.00 g, 2.72 mmol), lithium chloride (0.074 g, 1.66 mmol) and bis(triphenylphosphine)-palladium(II) chloride (0.203 g, 0.287 mmol) in toluene (7 mL) was degassed *via* five freeze–pump–thaw cycles and then heated at reflux under an atmosphere of N_2 for 72 h. After cooling, a saturated aqueous solution of potassium fluoride (10 mL) was added and the mixture stirred for 30 min. The insoluble residue formed was removed by filtration and washed with toluene. The combined filtrate and washings were evaporated to dryness under reduced pressure. The residue was taken up into CH_2Cl_2 (3 × 50 mL) and washed with aqueous $NaHCO_3$ (1 M, 2 × 50 mL). The organic phase was dried over anhydrous Na_2SO_4 and evaporated to dryness. The brown residue was purified by chromatography on a silica gel, gradient elution using hexane/diethyl ether 90/10 → 50/50, giving the product as a white solid (0.146 g, 53%). ^1H NMR (400 MHz, DMSO-d6): $\delta_H = 8.83$ (2H, d, H^6), 8.68 (1H, s, $H^{2'}$), 8.39 (2H, dd, H^3), 8.27 (2H, ddd, H^4), 8.11 (2H, d, $^3J(^{19}F–^1H) = 10$, $H^{4'}$), 7.72 (2H, ddd, H^5). Anal. Calcd for $C_{16}H_1FN_2$: C, 76.79; H, 4.43; N, 11.19%. Found: C, 76.55; H, 4.46; N, 11.16%.

^1H NMR data of 5-methyl-1,3-di(2-pyridyl)benzene for comparison (400 MHz, $CDCl_3$): $\delta_H = 8.73$ (2H, d, H^6), 8.39 (1H, s, $H^{2'}$), 7.92 (2H, s, $H^{4'}$), 7.85 (2H, d, H^3), 7.77 (2H, td, H^4), 7.26 (2H, td, H^5), 2.54 (3H, s, CH_3) (Chart 2).

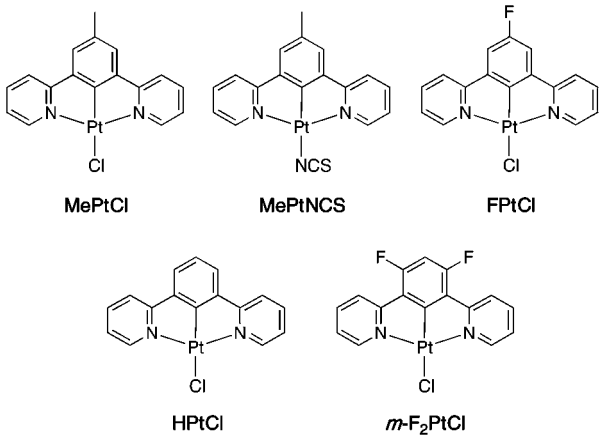

Chart 1 Structures of the complexes investigated (top) and of the unsubstituted and difluorinated analogues.

Synthesis of platinum(II) complexes

MePtCl. A solution of K_2PtCl_4 (337 mg, 0.815 mmol) in water (12.5 mL) was treated with a solution of 3,5-di(2-pyridyl)toluene (210 mg, 0.856 mmol) in acetonitrile (12.5 mL), and the mixture heated at reflux under N_2 for 3 days. After cooling to room temperature, the orange residue formed was collected by filtration and washed with water (2 × 20 mL) and ethanol (2 × 20 mL). After being dried under reduced pressure, the product was obtained as an orange-yellow solid (259 mg, 67% yield). ^1H NMR (400 MHz, $CDCl_3$): $\delta_H = 9.34$ (2H, d, $J(^{195}Pt)$ 38, H^6), 7.93 (2H, td, H^4), 7.66 (2H, d, $J(^{195}Pt)$ 6.3, H^3), 7.29 (2H, s, $H^{3'}$), 7.28 (2H, not fully resolved due to overlap with the former signal and solvent, m, H^5), 2.36 (3H, s, CH_3). ^1H NMR (400 MHz, CD_2Cl_2): $\delta_H = 9.29$ (2H, d, $J(^{195}Pt)$ 38, H^6), 8.00 (2H, td, H^4), 7.74 (2H, d, $J(^{195}Pt)$ 6, H^3), 7.39 (2H, s, $H^{3'}$), 7.35 (2H, ddd, H^5), 2.42 (3H, s, CH_3). MS FAB^+: 440 $(M - Cl)^+$. Anal. Calcd for $C_{17}H_{13}ClN_2Pt$: C, 42.91; H, 2.75; N, 5.89%. Found: C, 43.10; H, 2.86; N, 5.72% (Chart 3).

FPtCl. FPtCl was prepared similarly, in 60% yield. ^1H NMR (400 MHz, DMSO-d6): $\delta_H = 9.10$ (2H, d, $J(^{195}Pt)$ 32, H^6), 8.24 (2H, td, H^4), 8.17 (2H, d, H^3), 7.78 (2H, s, $J(^{19}F)$ 10, $H^{3'}$), 7.60 (2H, ddd, H^5). ^{13}C NMR (400 MHz, CD_2Cl_2): $\delta = 152.4$, 139.2, 123.8, 119.8, 111.5 (quaternary not detected). MS FAB^+: 444 $(M - Cl)^+$. Anal. Calcd for $C_{16}H_{10}ClFN_2Pt$: C, 40.05; H, 2.10; N, 5.83%. Found: C, 40.12; H, 2.10; N, 5.76%.

MePtNCS. Sodium thiocyanate (18 mg, 0.210 mmol) was added to a suspension of **MePtCl** (50 mg, 0.105 mmol) in methanol/acetone (5/20 v/v). The reaction mixture was stirred at room temperature for 1 day. The crude compound was dissolved in CH_2Cl_2, filtered, and precipitated twice from dry pentane, giving the pure product as a red solid (26 mg, 50% yield). ^1H NMR (400 MHz, CD_2Cl_2): $\delta_H = 8.77$ (2H, d, $J(^{195}Pt)$ 40, H^6),

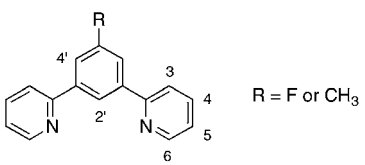

Chart 2 Numbering system for ^1H NMR assignment of ligands.

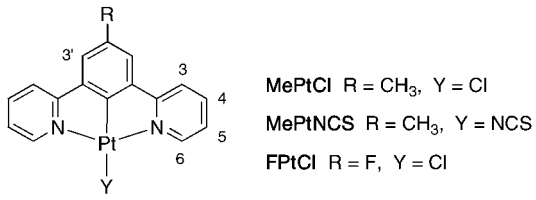

Chart 3 Numbering system for ^{1}H NMR assignment of complexes.

8.04 (2H, td, H^4), 7.73 (2H, d, J(^{195}Pt) 6, H^3), 7.36 (2H, ddd, H^5), 7.33 (2H, s, H$^{6'}$), 2.42 (3H, s, CH_3). ^{13}C NMR (400 MHz, CD_2Cl_2): δ = 152.3, 140.2, 124.9, 123.1, 119.1, 22.1 (CH_3) (quaternary not detected). IR (ν/cm^{-1}): for S***C****N*Pt, 2096 and 2089 in $CHCl_3$ and Nujol, respectively. MS FAB$^+$: 440 (M − NCS)$^+$; MS MALDI-TOF (with LiCl): 505 (M + Li)$^+$. Anal. Calcd for $C_{18}H_{13}N_3PtS$: C, 43.37; H, 2.63; N, 8.43%. Found: C, 43.57; H, 2.70; N, 8.52%.

Electrochemical measurements

Cyclic voltammetry was carried out using an Autolab PG-Stat 30 potentiostat with computer control and data storage *via* GPES Manager software. Solutions of concentration 1 mM in CH_2Cl_2 were used, containing [Bu_4N][PF_6] 0.1 M as the supporting inert electrolyte. A three-electrode assembly was employed, consisting of a platinum wire working electrode (0.012 cm^2), a platinum wire counter electrode and a saturated calomel electrode (SCE) as the reference electrode. The polishing procedure for the working Pt electrode consisted of surface cleaning with diamond powder (Aldrich, diameter 1 μm) on a wet cloth (DP-Nap, Struers). Solutions were purged for 5 min with solvent-saturated N_2 gas with stirring, prior to measurements being taken without stirring. The ohmic drop (310 Ω) was compensated by the positive feedback technique. The voltammograms were referenced to a ferrocene–ferrocenium couple as the standard ($E^{1/2}$ = 0.42 *vs.* SCE).

Photophysical measurements

Absorption spectra were measured on a Biotek Instruments XS spectrometer, using quartz cuvettes of 1 cm path length. Steady-state luminescence spectra were measured using a Jobin Yvon FluoroMax-2 spectrofluorimeter, fitted with a red-sensitive Hamamatsu R928 photomultiplier tube (PMT); the spectra shown are corrected for the wavelength dependence of the detector, and the quoted emission maxima refer to the values after correction. Samples for emission measurements were contained within quartz cuvettes of 1 cm path length, modified with appropriate glassware to allow connection to a high-vacuum line. Degassing was achieved *via* a minimum of three freeze–pump–thaw cycles whilst connected to the vacuum manifold; final vapour pressure at 77 K was $<5 \times 10^{-2}$ mbar, as monitored using a Pirani gauge. Luminescence quantum yields were determined relative to **MePtCl** as a secondary standard emitting in the same region.[5] The luminescence lifetimes of the complexes were measured by time-correlated single-photon counting, following excitation at 374 nm with an EPL-375 pulsed-diode laser. The emitted light was detected at 90° using a Peltier-cooled R928 PMT after passage through a monochromator. The estimated uncertainty in the quoted lifetimes is ±10% or better. Bimolecular rate constants for quenching by molecular oxygen, $k_Q^{O_2}$, were determined from the lifetimes in degassed and air-equilibrated solution, taking the concentration of oxygen in CH_2Cl_2 at 0.21 atm O_2 to be 2.2 mmol dm^{-3}.[20]

Device fabrication and characterization

Glass substrates coated with indium tin oxide (ITO) were cleaned ultrasonically in distilled water, acetone and 2-propanol. Subsequently, a 50 nm layer of poly(3,4-ethylene-dioxythiophene)/poly(styrenesulfonate) (PEDOT:PSS) (H.C. Starck Clevios P VP.AI 4083) was spin-coated from a water solution filtered through nylon (pore size 0.45 μm), and annealed at 100 °C for 10 min under a N_2 atmosphere. In the case of the green-emitting OLEDs (5% dopant in the emissive layer), a film of poly(*N*-vinylcarbazole) (PVK-h, average $M_w = 10^6$ g mol^{-1}) was then spin-coated from CH_2Cl_2 solution (12 mg mL^{-1}) onto the layers prepared as above. The samples were annealed at 150 °C for 30 min. The emitting layer, consisting of PVK-l (M_w = 42 000 g mol^{-1}),[21] 2-(4-biphenylyl)-5-(4-*tert*-butylphenyl)-1,3,4-oxadiazole (PBD), and either **FPtCl**, **MePtNCS** or **MePtCl**, was then spin-coated from a deaerated CH_2Cl_2 solution (8 mg mL^{-1}) comprised of 65% PVK-l:30% PBD:5% Pt complex by mass. The average total thickness of PVK-h and the emitting layer was equal to 165 nm for all three devices. Finally barium (5 nm layer) and aluminium (60 nm layer) were deposited by thermal vacuum evaporation at 10^{-6} mbar.

For the WOLED, a film of PVK-h mixed with poly(9,9-dioctylfluorenyl-2,7-diyl) end-capped with *N*,*N*-bis(4-methylphenyl)-4-aniline (PFO, American Dye Source), with ratio 52% PVK-h : 48% PFO by mass, was spin-coated from toluene solution (15 mg mL^{-1}) onto the PEDOT:PSS-covered ITO substrates. Samples were successively annealed at 100 °C for 30 minutes. Then the second layer, comprised of 40% PVK-l, 20% PBD, 40% **FPtCl** by mass, was spin-coated from CH_2Cl_2 solution (2 mg mL^{-1}). Finally calcium (10 nm layer) and aluminium (60 nm) were deposited by thermal vacuum evaporation at 10^{-6} mbar.

Electroluminescence (EL) and photoluminescence (PL) spectra of the devices were recorded using a liquid-nitrogen-cooled CCD camera in conjunction with a monochromator (Spex 270M). The light source for PL was a monochromated xenon lamp. The spectra were corrected for the instrument response functions. Current–voltage (*I*–*V*) device characterization was performed with a Keithley 2602 source meter combined with a calibrated photodiode. External quantum efficiency (EQE) was calculated by measuring the light emitted in the forward direction with Lambertian source assumption.[22] Device preparation and characterization was performed under a N_2 atmosphere inside a M-Braun glovebox system. CCT was evaluated according to ref. 23. Luminance (L), luminance efficiency (LE) and power efficiency (PE) were calculated using formulae from ref. 24.

AFM investigations were performed with a NT-MDT NTEGRA instrument in non-contact mode under ambient conditions.

Results and discussion

Synthesis of ligands and complexes

The ligand 5-fluoro-1,3-di(2-pyridyl)benzene was easily obtained by a Stille reaction of 1,3-dibromo-5-fluorobenzene with 2-(tri-*n*-butylstannyl)pyridine (molar ratio 1 : 2.5) in the presence of lithium chloride and bis(triphenylphosphine)-palladium(II) chloride as the catalyst, in toluene at reflux under N_2. Further reaction with K_2PtCl_4 in refluxing CH_3CN/H_2O (v/v) affords **FPtCl**.[7] Reaction of the known complex **MePtCl**[5] with NaSCN gives the new isothiocyanate Pt(II) complex, **MePtNCS**. The bonding of the SCN^- ligand to the Pt ion through the N atom is confirmed by the strong, sharp peak at 2096 cm^{-1} in $CHCl_3$ (2089 cm^{-1} in Nujol) a value typical of the $\nu(SCN)$ stretching mode of metal N-bonded isothiocyanate ligands[25] (see Experimental section and Scheme 1).

Photophysical and electrochemical properties in solution

Photophysical and electrochemical data for **FPtCl**, **MePtNCS** and **MePtCl** in solution are reported in Table 1. Their electronic absorption and photoluminescence spectra in diluted dichloromethane are complex, we attribute the intense absorption bands at $\lambda < 300$ nm to $^1\pi$–π^* transitions localized on the ligands, while those between 320 nm and 450 nm correspond to transitions of mixed charge-transfer/ligand-centred character.[5,6] A very weak band appears at around 490 nm, due to the formally forbidden $S_0 \rightarrow T_1$ transition facilitated by the high spin–orbit coupling associated with the platinum ion. The PL spectrum of complex **FPtCl** is essentially identical to that of **MePtCl**. It displays a vibrationally structured spectrum, $\nu \approx 1300$ cm^{-1}, with the 0,0 vibrational component at 504 ± 1 nm, representing a red-shift of 13 nm compared to the unsubstituted complex **HPtCl**.[5] This contrasts with the effect of fluorine atoms at the positions *meta* to the Pt ion in ***m*-F$_2$PtCl** (structures in Chart 1), as opposed to the *para*-disposed F atom in **FPtCl**. In ***m*-F$_2$PtCl**, the emission is *blue*-shifted by 20 nm compared to **HPtCl**.[26]

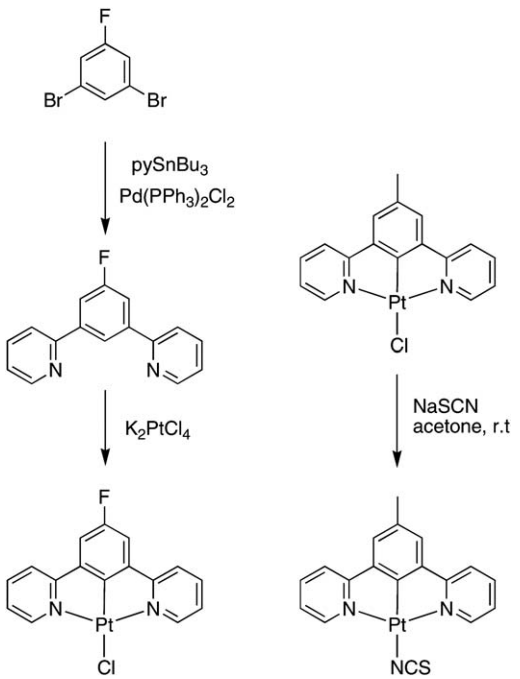

Scheme 1 Synthesis of the complexes **FPtCl** and **MePtNCS**.

These contrasting effects of the F atoms can be understood in terms of the frontier orbitals in such complexes. Thus, time-dependent density functional theory calculations on **HPtCl** have revealed that the T_1 state has predominantly HOMO–LUMO character.[27] The HOMO is based primarily on the aryl ring, the metal ion and the chloride co-ligand, whilst the LUMO is predominantly localised on the pyridyl rings. The inductive electron-withdrawing effect of F atoms, irrespective of whether they be *meta* or *para* to the metal, should lower the energy of both HOMO and LUMO, as found, for example, with iridium (III) complexes containing related fluorine-substituted terdentate ligands.[28] However, when the F atom is *para* to the metal as in **FPtCl**, the mesomeric electron-donating effect of F through the π orbitals will slightly attenuate the inductive effect. In contrast, there is no such possibility in ***m*-F$_2$PtCl**, in which the F atoms are *meta* to the metal, so the HOMO is expected to drop further in energy in this case. On the other hand, the extent to which the LUMO is stabilised in the latter complex may be expected to be slightly less than in the former, owing to the pyridyl rings (on which the LUMO is localised) being *ortho* to the F atoms, and therefore subject to the opposing mesomeric effect. These combined effects—which are represented schematically in Fig. S6 of the ESI‡—lead to the net trend in energies: **FPtCl** < **HPtCl** < ***m*-F$_2$PtCl**.

Meanwhile, the change in the monomeric co-ligand from chloride in **MePtCl** to isothiocyanate in **MePtNCS** is seen to have essentially no significant effect, probably reflecting the rather small participation of the co-ligand in such complexes,[27] and the similar positions of the NCS and Cl ligands in the spectrochemical series.

The relatively long lifetimes of several microseconds (Table 1) are typical of the phosphorescence of complexes of this class. The quantum yields of **FPtCl** and **MePtNCS** in degassed dichloromethane at room temperature were 0.47 and 0.60, comparable with those of **MePtCl** (see Table 1) and other complexes of this type.[6] That such high quantum yields arise despite the relatively long lifetimes (which are indicative of relatively low radiative rate constants) indicates that non-radiative decay processes in these complexes are particularly ineffective, probably reflecting the high rigidity of the system and high ligand-field strength associated with the *N^C^N*-coordinated ligand. The radiative k_r and non-radiative Σk_{nr} decay constants can be estimated from the lifetimes and quantum yields, assuming that the emitting state is formed with unitary efficiency (see footnote to Table 1). The rates of both processes are smaller than those typically found for more commonly studied iridium(III)-based OLED emitters,[29] for example, but the fact that the values are comparable to one another leads to the PL quantum yields of around 0.5.

The influence of increasing concentration on the absorption and PL spectra of **FPtCl** in dichloromethane is shown in Fig. 1 (b). While the shape of the absorption spectrum does not change, the PL spectra of all three complexes at higher concentrations reveal the appearance of a broad, structureless band at longer wavelengths, due to emission from an excimer, as observed for other members of this family of complexes.[5,6] The associated self-quenching rate constants of the monomer emission, k_Q^{SQ}, are of

Table 1 Photophysical and electrochemical parameters at 298 K in dichloromethane

	Absorption λ_{max}/nm (ε/L mol^{-1} cm^{-1})	Emission λ_{max}/nm	Φ_{lum}[a]	τ_0[b]/μs degassed (aerated)	$k_Q^{SQ}/10^9$ M^{-1} s^{-1}[b]	$k_Q^{O_2}/10^8$ M^{-1} s^{-1}[c]	k_r (Σk_{nr})/ 10^4 s^{-1}[d]	E_p^{red}[e]/ V	E_p^{ox}[e]/ V	HOMO[f]/ eV	LUMO[f]/ eV
MePtCl[g]	335 (5710) 381 (6900) 412 (6780) 460 (190) 495 (130)	505, 539, 578	0.68	7.8 (0.3)	3.3	16	8.7 (4.1)	−2.27[h]	0.36[h]	−5.16[h]	−2.53[h]
FPtCl	322sh (6170) 377 (7740) 422 (8270) 486 (312)	504, 542, 580	0.47	6.3 (0.6)	5.6	7.4	7.4 (8.5)	−2.19	0.56	−5.36	−2.61
MePtNCS	333 (4760) 357 (2800) 382 (3890) 406 (3820) 499 (188)	501, 533, 580	0.60	8.6 (0.7)	8.9	6.2	7.0 (4.6)	−2.21	0.24	−5.04	−2.59

[a] Luminescence quantum yield in degassed solution. [b] τ_0 is the lifetime at infinite dilution and k_Q^{SQ} the self-quenching rate constant, determined from the intercept and slope, respectively, of a plot of the measured emission decay rate constant against concentration. [c] Bimolecular rate constant for quenching by molecular oxygen, estimated using the lifetimes in degassed and air-equilibrated solutions, and taking $[O_2] = 2.2 \times 10^{-3}$ M in CH_2Cl_2 at 1 atm pressure of air. [d] Estimates of radiative k_r and non-radiative (Σk_{nr}, in parenthesis) decay constants are made as follows: $k_r = \Phi_{lum}/\tau_0$. $\Sigma k_{nr} = (1/\tau_0) - k_r$. [e] All processes were electrochemically irreversible, hence E_p^{ox} and E_p^{red} refer to peak potentials of oxidation and reduction, respectively; values are reported relative to a ferrocenium/ferrocene (Fc^+/Fc) redox couple used as an internal reference ($E^{1/2} = +0.42$ V *vs.* saturated calomel electrode SCE); at 298 K, in the presence of 0.1 M [Bu_4N][PF_6] as the supporting electrolyte, scan rate 200 mV s^{-1}. [f] Energies of the highest occupied molecular orbital HOMO and lowest unoccupied molecular orbital LUMO as calculated from the redox potentials. [g] Data from ref. 5 and 6. [h] Data from the present work.

a comparable magnitude in each case, as are the bimolecular oxygen quenching rate constants, which show only small differences amongst the three complexes.

A comparison of the cyclic voltammetry data for complexes **FPtCl**, **MePtNCS** and **MePtCl** is given in Table 1. As expected for the higher electron withdrawing effect of F with respect to a methyl group, **FPtCl** is more easily reduced and more difficult to oxidize with respect to **MePtCl**. The first oxidation and reduction potentials can be used to estimate the HOMO and LUMO energy levels by means of equations E_{HOMO} (eV) = $-(E_{OX} + 4.8)$ and E_{LUMO} (eV) = $-(E_{RED} + 4.8)$, which involve the use of the internal ferrocene standard value of −4.8 eV with respect to the vacuum level.[30] The HOMO–LUMO gap is 2.45, 2.63, and 2.75 eV for **MePtNCS**, **MePtCl**, and **FPtCl**, respectively (Table 1).

Spin-coated OLEDs using new Pt(II) complexes

Using complexes **FPtCl** and **MePtNCS** as phosphorescent dopants, we fabricated solution-processed multilayer electroluminescent devices with a typical composition of 100% PVK-h in the first layer and 65% PVK-l:30% PBD:5% Pt complex in the emissive layer. The PEDOT:PSS layer, which is standardly used in polymer based OLEDs, is considered as a part of the substrate. The chemical structures of the organic materials used are shown in Chart 4. The multilayer OLED approach has many advantages in comparison to single layer devices, but usually requires the use of thermal evaporation which is generally an expensive process. Here, we combined the simplicity of the low-cost spin-coating technique with the advantages of multilayer architecture. A PVK-h layer, directly deposited on PEDOT:PSS, plays a multiple role in our OLEDs. This polymer is well known as a hole transporting material,[31] and additionally is able to block the radiative excitons from direct quenching by PEDOT:PSS, removing a non-radiative decay channel introduced by this latter material.[22] High molecular weight PVK-h ($M_w = 10^6$ g mol^{-1}), with diminished solubility upon thermal treatment, allows us to fabricate multilayer architecture by successive solution deposition, as verified by AFM investigation. The top (emissive) layer is composed of the platinum complex dispersed in a host matrix comprised of PVK-l:PBD. PBD is an electron-transporting material, introduced in order to improve the balance between charges.

The EL spectra of OLEDs prepared in this way are shown in Fig. 2 together with HOMO and LUMO levels of used materials, and device performance data are compiled in Table 2. The EL spectra are similar to the corresponding PL spectra of dilute solutions. However, an additional long-wavelength component is evident, around 600 nm, superimposed on the emission of the complex and increasing in intensity in the order **FPtCl** < **MePtCl** < **MePtNCS**. This low-energy emission is attributed to a PVK electromer,[32] rather than to complex luminescence. The order of increasing intensity of the electromer can be explained by the charge-trapping properties of the complexes.

If a complex does not trap the charge carriers efficiently, they can travel into the host more freely and the probability that they will recombine on PVK-l:PBD matrix increases.

Poorer trapping ability of a complex will lead to a more intense electromer band being observed. In contrast, efficient trapping on a complex emitting centre will favour high EQE of devices[16] and also should decrease leakage current. In the present case, **FPtCl** doped in PVK-l:PBD host matrix has the best trapping abilities while **MePtNCS** has the poorest (see inset in Fig. 2), according to the trend in electromer intensities, and indeed this order is reflected in the EQE values in Table 2.

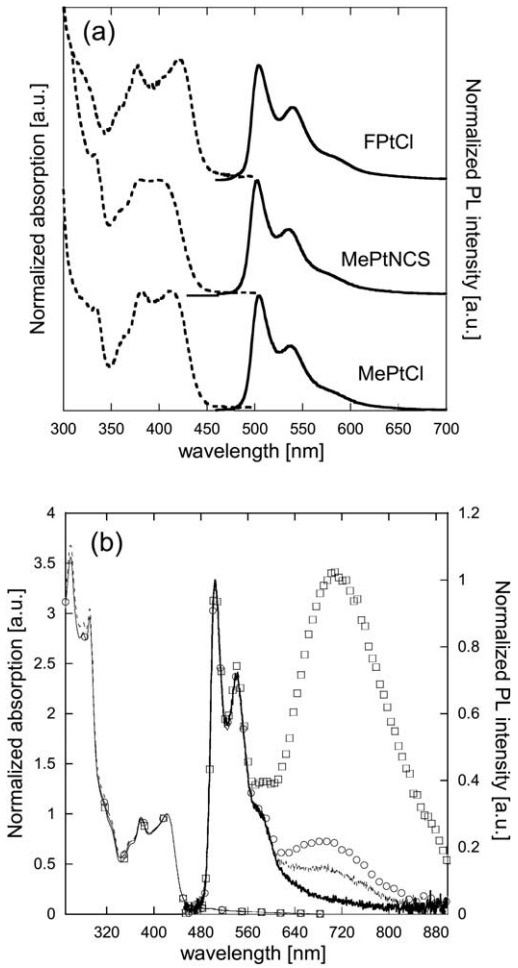

Fig. 1 (a) Absorption and PL spectra of **FPtCl**, **MePtNCS** and **MePtCl** in dichloromethane; (b) Absorption and PL spectra of **FPtCl** in dichloromethane at concentrations 4.15×10^{-5} M (solid line), 2.075×10^{-4} M (dashed line), 4.15×10^{-4} M (circles), and 2.075×10^{-3} M (squares).

It is remarkable that the EQE values obtained for the various devices (Table 2), although unsurprisingly lower than those obtained for OLEDs based on complexes of the same family built by evaporation techniques,[9] are one order of magnitude higher than for a recently reported OLED based on a substituted 4,4′-stilbenoid *N^C^N* platinum(II), also built by the spin-coating technique.[33]

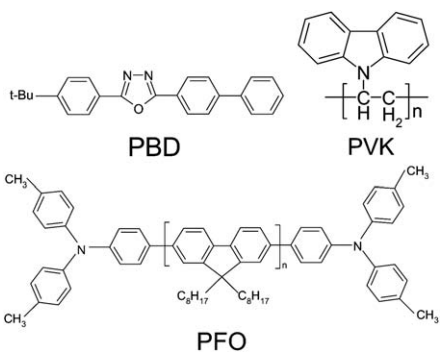

Chart 4 Molecular structures of PBD, PVK and PFO.

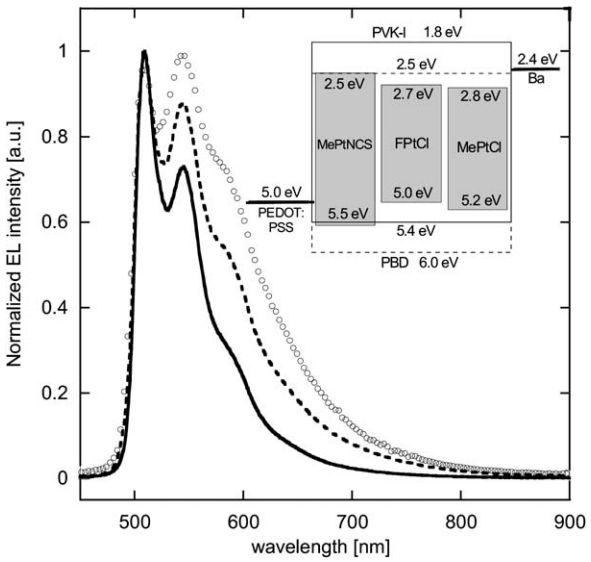

Fig. 2 EL spectra of PVK-h/65% PVK-l:30% PBD:5% Pt complex diodes:**FPtCl** (solid), **MePtCl** (dash), **MePtNCS** (circle). In the inset HOMO and LUMO levels of used materials are shown.

Table 2 Electroluminescence performance of devices based on **FPtCl**, **MePtNCS** and **MePtCl** with the device structure PVK-h/65% PVK-l:30% PBD:5% Pt complex

	FPtCl	**MePtNCS**	**MePtCl**
V_{on}/V	12	15	18
EQE[a] (%)	0.28	0.21	0.23
L[b]/cd m^{-2}	91	17	21
LE[b]/cd A^{-1}	0.94	0.62	0.68
PE[b]/lm W^{-1}	0.18	0.11	0.097
L_{max}/cd m^{-2}	755	161	195
CIE (x, y)	(0.32, 0.61)	(0.39, 0.55)	(0.37, 0.58)

[a] Maximum external quantum efficiency at the forward direction. [b] At a maximum external quantum efficiency.

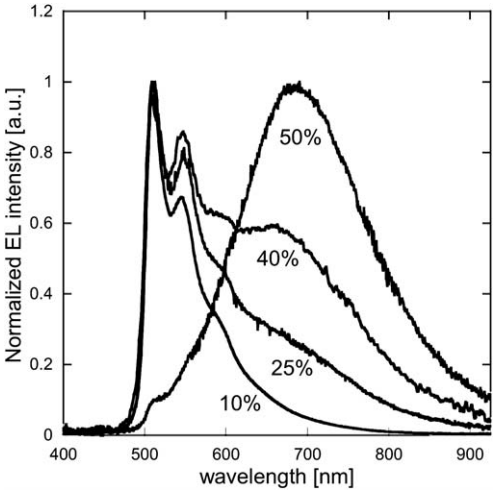

Fig. 3 EL spectra of single layer devices with different concentrations of **FPtCl** dispersed in PVK-l:PBD matrix.

By increasing the concentration of the **FPtCl** complex in the PVK-l:PBD matrix, we were able to tune the emission of the single layer devices (in this case without PVK-h bottom layer) from green to red (see Fig. 3), owing to the appearance of an excimer band centred at 700 nm. For the diode with the composition 40% PVK-l:20% PBD:40% **FPtCl**, balanced green and red emission was observed, and the same composition was therefore employed for the construction of a multilayer WOLED, as described in the next section.

WOLED

In this section, we present a multilayer WOLED prepared using a simple solution-processing technique. As diodes with a bottom layer consisting of PVK-h or PVK-h:PBD did not emit in the blue region, we introduced PFO (Chart 4) as an efficient blue emitter.[34] The selected structure for the device was: ITO/PEDOT:PSS/52% PVK-h:48% PFO/40% PVK-l:20% PBD:40% **FPtCl**/Ca/Al. A schematic diagram illustrating the HOMO and LUMO levels of each of the materials used is shown in Fig. 4. The bottom layer consists of a mixture of PVK-h and PFO, and serves as a blue-emitting and hole-transporting layer. PFO is known to provide good hole mobility.[35] Additionally, the HOMO level of PVK-h is lower compared to the PEDOT:PSS level, which facilitates injection of holes from the anode to PFO. The top layer is composed of the platinum complex **FPtCl** dispersed in PVK-l:PBD matrix. **FPtCl** is an effective hole-trapping centre (Fig. 4), collecting holes that arrive from the bottom layer and preventing their migration towards the cathode, automatically decreasing leakage current.

Fig. 5(a) shows the EL spectrum of the device, with Commission Internationale de l'Eclairage (CIE) coordinates $x = 0.28$, $y = 0.35$ and CCT equal to 8145 K, CRI equal 74 and EQE of about 4×10^{-4}%. The shoulder around 400–420 nm is most likely due to the residual emission of PFO α-phase,[36–38] almost eliminated after thermal treatment of the PVK-h:PFO layer (see Experimental part). The sharp peaks at 438 nm and 465 nm are due to the vibrational $0 \rightarrow 0$ and $0 \rightarrow 1$ components of the emission of the newly formed β phase PFO. In our diode, the emitted blue light can exit the device immediately or after reflection from the cathode. In the second case, partially absorbed light is used to excite the Pt(II) complex by an energy transfer process,[39,40] enabled by the overlap of the absorption of the complex and blue emitter's emission spectrum (Fig. 5(b)). Two-colour emission was obtained with a high concentration of **FPtCl** in the top layer. Bands at 509 nm and 544 nm, together with a shoulder at 590 nm, originate from the phosphorescence of single **FPtCl** molecules. The tail at low energy is due to complex excimer emission. The lower intensity of the excimer band observed in this WOLED in comparison to the single-emitting-layer device with the same concentration of the complex, described in the previous section, is probably caused by the partial dissolution of the bottom layer during preparation on the second film, as confirmed by AFM investigation. In this process, the effective dispersion of the complex at the interface is increased, changing the balance between accessible monomer and dimer states. The combined EL from the two layers creates white light, since green-red light emitted from the top layer is not absorbed by polymers in the bottom layer and thus exits the device freely, along with blue light from the bottom layer.

The corresponding PL spectrum of the device is also shown in Fig. 5(a). A difference in the green-red region can be noticed, with reversed intensities of monomer and excimer emission

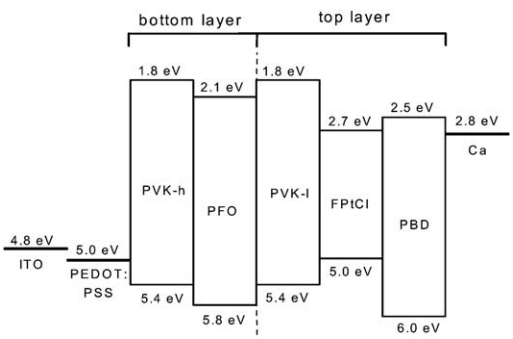

Fig. 4 Energy levels of materials used in the multilayer WOLED device.

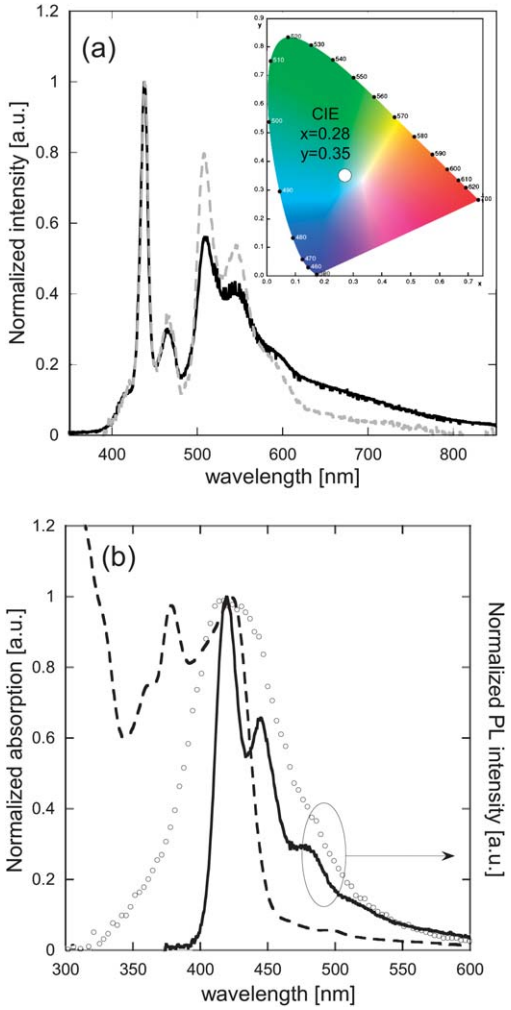

Fig. 5 (a) Comparison between EL at 7 V (solid) and PL ($\lambda_{exc} = 325$ nm, dashed) spectra of the diode of architecture ITO/PEDOT:PSS/52% PVK-h:48% PFO/40% PVK-l:20% PBD:40% **FPtCl**/Ca/Al. The inset shows the CIE coordinates of the EL spectrum. (b) Absorption spectrum of **FPtCl** in dichloromethane (dashed line) and PL spectra of films of PFO (solid line) and PBD:PVK-l (circles). Excitation wavelengths were 325 nm and 320 nm for PFO and PVK-l:PBD, respectively.

compared to EL. Such a discrepancy between EL and PL originates from the different mechanisms responsible for the exciton and excimer generation in two types of luminescence. In PL, energy transfer is the dominant phenomenon, while in EL, the charge trapping properties of the system are the main contributor. PFO emission recorded in EL suggests that electrons may enter into the bottom layer and bind there some holes on emitting centres localized on PFO. In devices with a bottom layer consisting of PVK-h or PVK-h:PBD, blue EL is not observed. This is due to the good transporting properties of both materials, preventing efficient trapping of charge carriers on emitting centres, and to their emission quantum yields being only modest.[41] On the other hand, PFO is an efficient emitter and is able to trap electrons in the PFO:PVK-h system in the bottom layer (see Fig. 4).

Conclusions

We have synthesized two phosphorescent green-emitting *N^C^N*-coordinated platinum(II) complexes, **FPtCl** and **MePtNCS**, and we have compared their properties with those of **MePtCl**. Photophysical measurements revealed that, in addition to green emission, the complexes also display an excimer band centred around 700 nm. The emitters were tested in simple-to-build, solution-processable OLEDs as dopants in a PVK:PBD matrix. The obtained external quantum efficiencies were ten times higher than for a recently reported OLED based on a substituted 4,4′-stilbenoid *N^C^N* platinum(II), also built by the spin-coating technique. The more promising **FPtCl**, thanks to its double emission color, was used as a single dopant in solution processed multilayer WOLED. Green and red light originated from the monomer and excimer emission of the complex, respectively, while blue came from the bottom layer. Application of highly concentrated dopant displaying excimer emission allows the device structure to be simplified, as energy transfer between multiple dopants is reduced. Additionally we combined the facility of the low-cost spin-coating technique with the advantages of multilayer architecture. The study reveals that the Pt(*N^C^N*) class of emitters are amenable to the production of solution-processed OLEDs, in addition to the vacuum-sublimed systems mostly investigated to date for such compounds, which are more costly and therefore less suitable for large areas.

Acknowledgements

We deeply thank Dr Luigi Falciola (Dip. di Chimica Fisica ed Elettrochimica dell'Università degli Studi di Milano) for electrochemical measurements and Dr Andrea Arcari for development of a setup for OLED characterization. This work was supported by the CARIPLO Foundation (2007, Diodi per illuminazione a luce bianca basati su nuovi complessi organometallici), by MIUR (FIRB 2004: RBPR05JH2P and PRIN 2008: 2008FZK5AC002) and by COST Action D35.

Notes and references

1 M. A. Baldo, D. F. O'Brien, Y. You, A. Shoustikov, S. Sibley, M. E. Thompson and S. R. Forrest, *Nature*, 1998, **395**, 151.
2 *Highly Efficient OLEDs with Phosphorescent Materials*, ed. H. Yersin, Wiley-VCH, Berlin, 2007.
3 (*a*) For reviews, see for example: D. R. McMillin and J. J. Moore, *Coord. Chem. Rev.*, 2002, **229**, 113; (*b*) S.-W. Lai and C.-M. Che, *Top. Curr. Chem.*, 2004, **241**, 27; (*c*) B. Ma, P. Djurovich and M. E. Thompson, *Coord. Chem. Rev.*, 2005, **249**, 1501; (*d*) F. N. Castellano, I. E. Pomestchenko, E. Shikhova, F. Hua, M. L. Muro and N. Rajapakse, *Coord. Chem. Rev.*, 2006, **250**, 1819; (*e*) K. M.-C. Wong and V. W.-W. Yam, *Coord. Chem. Rev.*, 2007, **251**, 2477; (*f*) J. A. G. Williams, *Top. Curr. Chem.*, 2007, **281**, 205; (*g*) J. A. G. Williams, S. Develay, D. L. Rochester and L. Murphy, *Coord. Chem. Rev.*, 2008, **252**, 2596; (*h*) W.-Y. Wong and C.-L. Ho, *J. Mater. Chem.*, 2009, **19**, 4457; (*i*) J. A. G. Williams, *Chem. Soc. Rev.*, 2009, **38**, 1783; (*j*) A. F. Rausch, H. H. H. Homeier and H. Yersin, *Top. Organomet. Chem.*, 2010, **29**, 193.
4 D. J. Cardenas, A. M. Echavarren and M. C. Ramirez de Arellano, *Organometallics*, 1999, **18**, 3337.
5 J. A. G. Williams, A. Beeby, E. S. Davies, J. A. Weinstein and C. Wilson, *Inorg. Chem.*, 2003, **42**, 8609.
6 (*a*) S. J. Farley, D. L. Rochester, A. L. Thompson, J. A. K. Howard and J. A. G. Williams, *Inorg. Chem.*, 2005, **44**, 9690; (*b*) A. Rausch, L. Murphy, J. A. G. Williams and H. Yersin, *Inorg. Chem.*, 2009, **48**, 11407.
7 Z. Wang, E. Turner, V. Mahoney, S. Madakuni, T. Groy and J. Li, *Inorg. Chem.*, 2010, **49**, 11276.
8 W. Sotoyama, T. Satoh, N. Sawatari and H. Inoue, *Appl. Phys. Lett.*, 2005, **86**, 153505.
9 M. Cocchi, D. Virgili, V. Fattori, D. L. Rochester and J. A. G. Williams, *Adv. Funct. Mater.*, 2007, **17**, 285.
10 V. Adamovich, J. Brooks, A. Tamayo, A. M. Alexander, P. I. Djurovich, B. W. D'Andrade, C. Adachi, S. R. Forrest and M. E. Thompson, *New J. Chem.*, 2002, **26**, 1171.
11 B. W. D'Andrade and S. R. Forrest, *Adv. Mater.*, 2004, **16**, 1585.
12 B. W. D'Andrade, *Nat. Photonics*, 2007, **1**, 33.
13 J.-H. Jou, M.-H. Wu, S.-M. Shen, H.-C. Wang, S.-Z. Chen, S.-H. Chen, C.-R. Lin and Y.-L. Hsieh, *Appl. Phys. Lett.*, 2009, **95**, 013307.
14 J.-H. Jou, C.-P. Wang, M.-H. Wu, H.-W. Lin, H. C. Pan and B.-H. Liu, *J. Mater. Chem.*, 2010, **20**, 6626.
15 (*a*) B. W. D'Andrade, J. Brooks, V. Adamovich, M. E. Thompson and S. R. Forrest, *Adv. Mater.*, 2002, **14**, 1032; (*b*) B. Ma, P. I. Djurovich, S. Garon, B. Alleyne and M. E. Thompson, *Adv. Funct. Mater.*, 2006, **16**, 2438.
16 E. L. Williams, K. Haavisto, J. Li and G. E. Jabbour, *Adv. Mater.*, 2007, **19**, 197.
17 G. Zhou, Q. Wang, X. Wang, C.-L. Ho, W.-Y. Wong, D. Ma, L. Wang and Z. Li, *J. Mater. Chem.*, 2010, **20**, 7472.
18 M. Cocchi, J. Kalinowski, L. Murphy, J. A. G. Williams and V. Fattori, *Org. Electron.*, 2010, **11**, 388.
19 J. Kalinowski, M. Cocchi, D. Virgili, V. Fattori and J. A. G. Williams, *Adv. Mater.*, 2007, **19**, 4000.
20 M. Montalti, A. Credi, L. Prodi and M. T. Gandolfi, *Handbook of Photochemistry*, CRC Press, Boca Raton, FL, 3rd edn, 2006.
21 PVK applied in bottom and top layers has the same optical and electrical properties, and differs only in molecular weight.
22 U. Giovanella, P. Betti, C. Botta, S. Destri, J. Moreau, M. Pasini, W. Porzio, B. Vercelli and A. Bolognesi, *Chem. Mater.*, 2011, **23**, 810.
23 C. S. McCamy, *Color Res. Appl.*, 1992, **17**, 142; J. Hernandez-Andres, R. L. Lee, Jr and J. Romero, *Appl. Opt.*, 1999, **38**, 5703.
24 H. Li, C. Zhang, D. Li and Y. Duan, *J. Lumin.*, 2007, **122–123**, 626.
25 (*a*) J. L. Burmeister and F. Basolo, *Inorg. Chem.*, 1964, **3**, 1587; (*b*) M. J. Coyer, M. Croft, J. Chen and R. H. Herber, *Inorg. Chem.*, 1992, **31**, 1752; (*c*) J. S. Field, C. D. Grimmer, O. Q. Munro and B. P. Waldron, *Dalton Trans.*, 2010, **39**, 1558.
26 M. Cocchi, J. Kalinowski, V. Fattori, J. A. G. Williams and L. Murphy, *Appl. Phys. Lett.*, 2009, **94**, 073309.
27 D. L. Rochester, S. Develay, S. Zalis and J. A. G. Williams, *Dalton Trans.*, 2009, 1728.
28 A. J. Wilkinson, H. Puschmann, J. A. K. Howard, C. E. Foster and J. A. G. Williams, *Inorg. Chem.*, 2006, **45**, 8685.
29 (*a*) L. Flamigni, A. Barbieri, C. Sabatini, B. Ventura and F. Barigelletti, *Top. Curr. Chem.*, 2007, **281**, 143; (*b*) J. A. G. Williams, A. J. Wilkinson and V. L. Whittle, *Dalton Trans.*, 2008, 2081.
30 R. S. Ashraf, M. Shahid, E. Klemm, M. Al-Ibrahim and S. Sensfuss, *Macromol. Rapid Commun.*, 2006, **27**, 1454; W.-Y. Wong, X.-Z. Wang, Z. He, A. B. Djurisic, C.-T. Yip, K.-Y. Cheung, H. Wang, C. S. K. Mak and W.-K. Chan, *Nat. Mater.*, 2007, **6**, 521.

31 F. C. Bos and D. M. Burland, *Phys. Rev. Lett.*, 1987, **58**, 152.
32 L. Qian, D. Bera and P. H. Holloway, *J. Chem. Phys.*, 2007, **127**, 244707.
33 G. D. Batema, M. Lutz, A. L. Spek, C. A. van Walree, C. de Mello Donegá, A. Meijerink, R. W. A. Havenith, J. Pérez-Moreno, K. Clays, M. Büchel, A. van Dijken, D. L. Bryce, G. P. M. van Klink and G. van Koten, *Organometallics*, 2008, **27**, 1690.
34 A. W. Grice, D. D. C. Bradley, M. T. Bernis, M. Inbasekaran, W. W. Wu and E. P. Woo, *Appl. Phys. Lett.*, 1998, **73**, 629.
35 M. Redecker, D. D. C. Bradley, M. Inbasekaran and E. P. Woo, *Appl. Phys. Lett.*, 1998, **73**, 1565.
36 A. J. Cadby, P. A. Lane, H. Mellor, S. J. Martin, M. Grell, C. Giebeler, D. D. C. Bradley, M. Wohlgenannt, C. An and Z. V. Vardeny, *Phys. Rev. B: Condens. Matter Mater. Phys.*, 2000, **62**, 15604.
37 M. Grell, D. D. C. Bradley, X. Long, T. Chamberlain, M. Inbasekaran, E. P. Woo and M. Soliman, *Acta Polym.*, 1998, **49**, 439.
38 M. Grell, D. D. C. Bradley, M. Inbasekaran and E. P. Woo, *Adv. Mater.*, 1997, **9**, 798.
39 T. Förster, *Discuss. Faraday Soc.*, 1959, **27**, 7.
40 J. R. Lakowicz, in *Principles of Fluorescence Spectroscopy*, Kluwer Academic/Plenum Publishers, New York, 2nd edn, 1999, ch. 1, pp. 13–14.
41 J. Mezyk, W. Mróz, A. Mech, U. Giovanella, F. Meinardi, C. Botta, B. Vercelli and R. Tubino, *Phys. Chem. Chem. Phys.*, 2009, **11**, 10152.